Photomedicine and Laser Surgery
Volume 34, Number 11, 2016

Pp. 556–563
DOI: 10.1089/pho.2015.4025

Mesenchymal Stem Cells Synergize with 635, 532, and 405 nm Laser Wavelengths in Renal Fibrosis: A Pilot Study

Megan O'Connor, MS,[1] Rachana Patil, MS,[1] Jiangzhou Yu, MD, PhD,[1]
Richard Hickey, BS,[1] Kavitha Premanand, MS,[1] Andre Kajdacsy-Balla, MD, PhD,[2]
Enrico Benedetti, MD,[1,3] and Amelia Bartholomew, MD, MPH, FACS[1]

Abstract

Objective: To address whether a single treatment of one of three visible light wavelengths, 635, 532, and 405 nm (constant wave, energy density 2.9 J/m^2), could affect the hallmarks of established renal fibrosis and whether these wavelengths could facilitate mesenchymal stem cell (MSC) beneficence. ***Background data:*** Chronic kidney disease is a global health problem with only 20% receiving care worldwide. Kidneys with compromised function have ongoing inflammation, including increased oxidative stress and apoptosis, peritubular capillary loss, tubular atrophy, and tubulointerstitial fibrosis. Promising studies have highlighted the significant potential of MSC-based strategies to mitigate fibrosis; however, reversal of established fibrosis has been problematic, suggesting that methods to potentiate MSC effects require further development. Laser treatments at visible wavelengths have been reported to enhance mitochondrial potential and available cellular ATP, facilitate proliferation, and inhibit apoptosis. We hypothesized that laser-delivered energy might provide wavelength-specific effects in the fibrotic kidney and enhance MSC responses. ***Materials and methods:*** Renal fibrosis, established in C57BL6 mice following 21 days of unilateral ureter obstruction (UUO), was treated with one of three wavelengths alone or with autologous MSC. Mitochondrial activity, cell proliferation, apoptosis, and cytokines were measured 24 h later. ***Results:*** Wavelengths 405, 532, and 635 nm all significantly synergized with MSC to enhance mitochondrial activity and reduce apoptosis. Proliferative activity was observed in the renal cortices following combined treatment with the 532 nm laser and MSC; endothelial proliferation increased in response to the 635 nm laser alone and to the combined effects of MSC and the 405 nm wavelength. Reductions of transforming growth factor-β were observed with 532 nm alone and when combined with MSC. ***Conclusions:*** Specific wavelengths of laser energy appear to induce different responses in renal fibrotic tissue. These findings support further study in the development of a customized laser therapy program of combined wavelengths to optimize MSC effects in the treatment of renal fibrosis.

Keywords: kidney fibrosis, laser wavelength, mesenchymal stem cell, tissue regeneration

Background

Chronic kidney disease is considered a worldwide health crisis; only 20% of affected individuals are treated worldwide.[1,2] The financial burden of ongoing treatment remains a significant obstacle to care. Strategies aimed at facilitating permanent endogenous recovery of kidney function may circumvent this obstacle. Kidneys with compromised function have developed structural changes in response to ongoing inflammation, including increased oxidative stress and apoptosis, peritubular capillary loss, tubular atrophy, and tubulointerstitial fibrosis.[3–5] Transforming growth factor-β (TGF-β) has been implicated as a key player in epithelial–mesenchymal transition, a process that contributes pathologically to fibrosis and excessive deposition of extracellular matrix.[6–8]

While mesenchymal stem cell (MSC) have shown to improve acute kidney injury, their effect in chronic fibrotic kidney disease has been less effective.[9] MSC have been reported to suppress some of the underlying inflammatory responses and oxidative stress associated with fibrosis, improve regulation of matrix deposition and remodeling, and inhibit the TGF-β pathway.[9–14] Encouraging findings have shown reduced albuminuria, collagen IV deposition, and loss of peritubular capillaries, but MSC alone could not completely reverse or restore function, despite their abilities to facilitate endothelial and epithelial proliferation.[15,16]

Departments of [1]Surgery, [2]Pathology, and [3]Transplant Surgery, University of Illinois at Chicago, Chicago, Illinois.

One possible explanation for the diminished responses to MSC in chronic kidney disease may be the limited amount of energy available to the cell during ongoing cell injury, a state that leads to a rapid depletion of cytoplasmic ATP.[17] With limited stores of energy, cells are unable to proliferate and instead adapt their metabolic activities to focus primarily on survival.[18] It is possible that repletion of cellular energy stores may enable cells to better respond to proliferative and regenerative signals delivered by MSC. Laser treatment at visible wavelengths has been reported to increase the cellular ATP content.[19–21] Enhanced availability of ATP has translated to increased cellular activities with reports of enhanced production of keratinocyte growth factor (KGF),[22] fibroblaster growth factor (FGF),[23] and hepatocyte growth factor (HGF)[24] by fibroblasts *in vitro* after treatment with 660, 632.8, and 532 nm, respectively. In clinical and veterinary treatments, laser-delivered energy of various visible wavelengths has been reported to treat acute muscle injury leading to the proregenerative findings of increased growth factors and enhanced angiogenesis.[25] These data suggest that deposition of energy, particularly to the ailing proximal tubular epithelial cells and peritubular endothelial cells that struggle to avoid apoptosis in the fibrotic kidney, may be able to arrest the progression to apoptosis and may provide enough available energy to initiate regenerative proliferative responses.

In the present study, we investigated the effect of a single treatment of one of three visible light wavelengths, 635, 532, and 405 nm (constant wave), alone or in combination with MSC for mitigation of ongoing renal fibrosis in a mouse unilateral ureteral obstruction model. To determine the effects of differential energy delivery, we investigated the frequency of mitochondrial activation, apoptosis, TGF-β tissue content, and cellular proliferation. To determine whether energy delivery would facilitate proregenerative responses to MSC, we investigated the possibility of synergistic effects between laser wavelength and MSC. The data showed laser treatments synergized with MSC to augment the beneficial effects of MSC; each wavelength contributed to either mitigation of activities associated with fibrosis or the proregenerative activities of mitochondrial activation and endothelial proliferation.

Materials and Methods

Animals

Male C57BL/6 mice, 12 weeks old, underwent right unilateral ureter obstruction (UUO) to induce renal parenchymal fibrosis.[26] Following ketamine/xylazine anesthesia, a 3 cm midline incision exposed the right kidney where the ureter was doubly ligated 3–4 mm below the renal pelvis. The abdomen was sutured closed and mice were allowed to recover for 3, 7, 14, or 21 days and then euthanized. All animals received humane care as per University of Illinois guidelines; all procedures were approved by the Animal Care Committee at the University of Illinois, IACUC # 12-096 and 15-094.

MSC isolation and expansion

MSC were prepared as we have described previously.[27] MSC were isolated from tibiae and femurs of 4-week-old mice, after marrow cells were plated at a concentration of 2×10^7 cells per 9.6 cm^2 in a 75-cm^2 flask with 20 mL MSC media (40% alpha-modified Eagle's medium, 40% F-12 nutrient mixture, 10% heat-inactivated fetal calf serum, and 1% antibiotic–antimycotic solution).[27] Nonadherent cells were discarded at 72 h, and adherent cells underwent negative selection using Miltenyi immunomagnetic beads coated with biotinylated antibodies to CD11b and CD45 (eBioscience, San Diego, CA). The resultant culture adherent cells were replated at 1×10^6 cells per 175-cm^2 flask and culture expanded to the fourth passage with <1% contamination with $CD45^+$ cells. MSC were administered intravenously using 100 μL Dulbecco's buffered saline (DBS).

Low-level light laser and MSC treatments

Twenty days after UUO (D20 UUO), mice were randomly assigned to eight treatment groups ($n=3$ per group); vehicle control (DBS), autologous MSC alone, 635, 532, or 405 nm laser with or without MSC. Low-level light laser treatment was administered through research-grade 17.5 mW diode laser (Laser Power Source box: Zerona Medical Laser, Model #: ERC-INV 00003; Erchonia Corporation, McKinney, TX) emitting 635, 532, or 405 nm through constant wave (Table 1). A 3-cm-radius area overlying the right kidney was irradiated with the desired wavelength for 300 sec anteriorly and posteriorly with the animal positioned 8 cm from the rotating laser source. MSC, 1×10^6 MSC, were administered intravenously immediately following the laser treatment. Animals underwent euthanasia 24 h following MSC administration.

Histology and immunofluorescence

Following euthanasia, the right kidneys were excised, divided, fixed in 4% paraformaldehyde in 0.1 M phosphate buffer, pH 7.4, paraffin embedded, and sections cut 3 μm thick. Parenchymal changes were examined by sections stained with hematoxylin and eosin (BBC Histo·Perfect H&E Staining System; BBC Biochemicals, Mount Vernon, WA). Masson's trichrome stain (NovaUltra Special Stain Kit; IHC World, Woodstock, MD) was used to identify and measure parenchymal fibrosis.

Mitochondrial activity. MitoTracker Red CMXRos, M7512 (1 mM solution, intravenously; Molecular Probes, Eugene, OR), was administered 30 min before euthanasia to be concentrated by active mitochondria and retained during cell fixation.[28] Following euthanasia, kidney tissues were immediately frozen in Tissue-Tek, and 4-μm-thick sections were mounted on glass slides, fixed in ice-cold methanol for 15 min at −20°C, and counterstained with DAPI solution (300 nM). The slides were imaged on the stage of an inverted microscope (Axiovert 100 M) using the 568 nm laser line for the red label and emission measured using a 585 nm filter.[29]

Endothelial proliferation. Twenty-four hours before euthanasia, BrdU, (10 mg/mL, 300 μL intramuscularly; Sigma-Aldrich, St. Louis, MO) was administered. Tissue sections were stained with the primary mouse Biotin anti-BrdU antibody (BrdU In-Situ Detection Kit; BD Pharmingen, San Jose, CA) and positively stained cells were expressed as an average count per high-power field of 20 high-power fields

Table 1. Irradiance Parameters for Low-Level Light Laser Treatments

Wavelength (nm)	*Operating mode*	*Peak radiant power (mW)*	*Beam shape/ spot size at target*	*Irradiance at skin level (8 cm from aperture) (mW/cm^2)*	*Exposure duration (sec)*	*Radiant exposure (mJ/cm^2)*	*Total radiant energy (mJ)*
405	CW	17.25 ± 1.25	Elliptical/1.413 cm^2	12.20	300	3.662	5.1748
532	CW	17.25 ± 1.25	Elliptical/1.413 cm^2	12.20	300	3.662	5.175
635	CW	17.25 ± 1.25	Elliptical/1.413 cm^2	12.20	300	3.662	5.175

CW, continuous wave.

surveyed (20×) per section. To differentiate between cortical or medullary regions, each slide underwent region delineation by hand with automated cell counts (Vectra Automated Quantitative Pathology Imaging System; CRi, Inc., TX) and analyzed by inForm analysis software. Proliferating endothelial cells were enumerated as the mean number of cells positively stained for both CD31 (Novus, Littleton, CO) and BrdU expressed as a percentage of the total positively stained $CD31^+$ cells per high-power field with 20 random high-power fields counted per section.

Apoptosis. TUNEL staining was performed for detection of apoptotic cells according to the manufacturer's instructions (DeadEnd Fluorometric TUNEL System; Promega Corporation, Madison, WI). Tissues samples from naive kidneys were used as negative control. TUNEL-positive nuclei were counted in a total of 20 random high-power fields. Images were acquired using Vectra and analyzed with inForm Software.

Immunoassays for TGF-β and IL-10

Weighed, cryopreserved renal tissue homogenates were used for the determination of active murine TGF-β1and IL-10 using ELISA (R&D Systems, Minneapolis, MN). These experiments were conducted as per the manufacturer's instructions. Values were expressed as pg/mg protein.

Statistical analysis

Statistical analysis was performed using Minitab Statistics (State College, PA). Data are expressed as mean ± SE. Significant difference among groups was determined by one-way analysis of variance or a two-tailed *t*-test where $p \leq 0.05$ was considered statistically significant.

Results

Renal architecture of the day 20 UUO model

Serial culls performed immediately after UUO, and on days 3, 7, 14, and 20 days demonstrated progressive enlargement of renal pelvises and calices with progressive thinning of the remaining cortex. Appreciable collagen staining was first detected on day 7 with significant increases by day 20 (Supplementary Fig. S1; Supplementary data are available online at www.liebertonline.com/pho). Renal tubules demonstrated progressive dilation and finally, obliteration and loss. Shrinkage of glomeruli, peritubular capillary endothelial loss, and expansion of Bowman's capsule were also observed at day 20. Initial influx of inflammatory mononuclear cells at day 7 diminished over time. These findings defined day 20 as a model of advanced renal parenchymal fibrosis.

MSC synergize with low-level light laser to enhance mitochondrial activity

Following laser treatment with or without MSC, we observed differentially increased mitochondrial activation, (Fig. 1A, B). The 635 nm wavelength significantly increased mitochondrial activity when compared to D20 UUO controls, (2.43 ± 0.45 vs. 0.60 ± 0.25, $p < 0.05$). The 532 and 405 nm wavelengths and MSC had modest effects as single modalities (1.32 ± 0.31 [532 nm], 1.50 ± 0.51 [405 nm], and 1.85 ± 0.41 [MSC]). Addition of MSC to each laser wavelength significantly exceeded the mitochondrial activity of the D20 UUO group, (5.00 ± 0.67, 6.53 ± 0.91, or 5.11 ± 0.90 vs. single modalities 635, 532, and 405 nm, respectively, $p < 0.05$). A pairwise comparison of each MSC-based laser treatment to its corresponding laser-alone group demonstrated significant increases with the addition of MSC, $p < 0.05$. These findings demonstrate a synergistic effect between each laser wavelength tested and MSC in enhancing mitochondrial activity in fibrotic renal parenchyma.

Reduced frequency of apoptosis

Renal fibrosis is associated with ongoing apoptosis and cell loss.[30,31] All three wavelengths and MSC alone significantly reduced the number of apoptotic cells observed when compared to the D20 UUO group control (Fig. 2A, B). Addition of autologous MSC to laser treatments did not enhance this effect, suggesting that no further gains in apoptosis reduction could be gained by combining treatments.

MSC synergize with the 532 nm wavelength to enhance proliferative activity in the renal cortex

Cell proliferation detected within fibrotic kidneys can be attributed to the small subpopulation of proximal renal tubule epithelial cells, which function as progenitor cells, with hematopoietic and MSC constituting extremely small populations, even after severe organ injury.[15,32–35] After division, proximal tubular cells become quiescent for at least 7 days.[36] Since proximal tubules reside exclusively in the cortex, the frequency of proliferating cells was categorized as either cortical or medullary. Of the two regions, the cortical region appeared to undergo a greater proliferative activity than the medulla (Fig. 3). None of the treatment

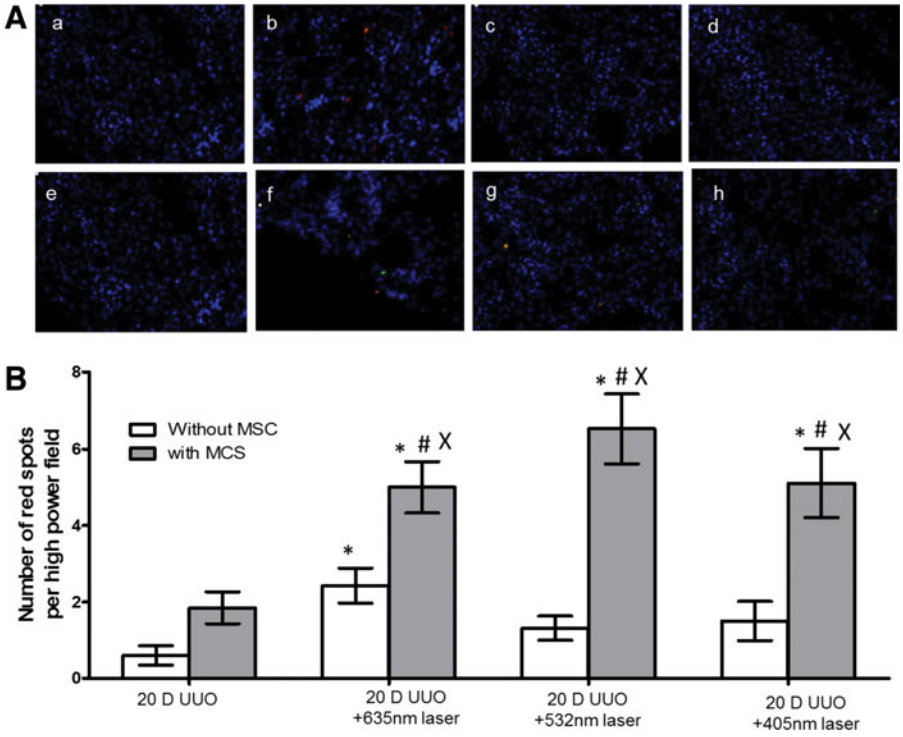

FIG. 1. Mitochondrial activity observed in the renal parenchyma following UUO-induced fibrosis and low-level light laser, MSC, or the two in combination. **(A)** Parenchyma stained with MitoTracker Red CMXRos is representative of 3 experiments with 20 high-power fields (20×) examined per animal and shows fibrotic kidney tissue alone **(a)** or treatment with laser with or without MSC as follows: **(b)** 635 nm laser, **(c)** 532 nm laser, **(d)** 405 nm laser. **(e)** MSC, **(f)** 635 nm laser with MSC, **(g)** 532 nm laser with MSC, **(h)** 405 nm laser with MSC. **(B)** ANOVA followed by paired *T* tests determined significance as follows: $^{*}p < 0.05$ versus 20 D UUO alone, $^{\#}p < 0.05$ versus 20 D UUO+MSC. $^{X}p < 0.05$ versus corresponding laser-treated UUO. 20 D, 20 days; ANOVA, analysis of variance; MSC, mesenchymal stem cells; UUO, unilateral ureter obstruction.

groups demonstrated enhanced proliferation in the medulla. In the cortex, there was a strong trend for 635 nm laser-enhanced proliferative activity (12.69% ± 2.97% vs. 4.50% ± 1.59% $BrdU^{+}$ cells per high-power field), however, the variability observed between animals precluded statistical significance. Analyses of each laser wavelength with MSC revealed that the combination of 532 nm with MSC was significantly better than UUO alone (28.88% ± 4.97% vs. 4.50% ± 1.59%, $p = 0.01$), than MSC alone (28.88% ± 4.97% vs. 11.43% ± 1.75%, $p = 0.04$), and better than the 532 laser alone (28.88% ± 4.97% vs. 5.15% ± 1.23%, $p = 0.01$). The 405 and 635 nm wavelengths also synergized with MSC and reached statistical significance.

MSC synergize with the 405 nm wavelength to enhance endothelial proliferative activity

Peritubular capillary loss is associated with tubular atrophy, tubular loss, and interstitial fibrosis.[37] Efforts to enhance endothelial proliferation through VEGF or other means have been shown to mitigate fibrosis.[38]To determine whether laser treatment enhanced the endothelial

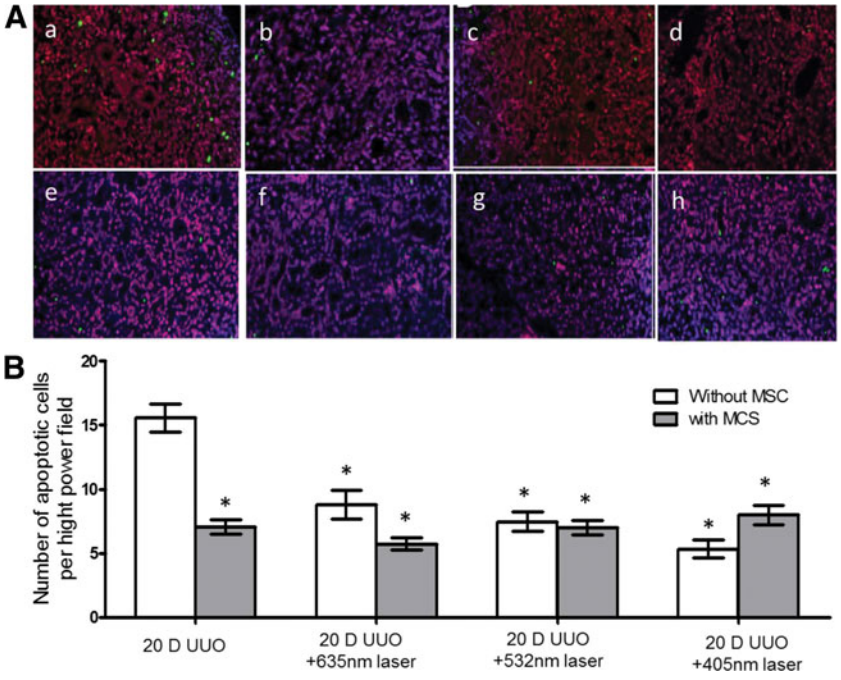

FIG. 2. Quantification of renal parenchymal apoptotic cells (green) following UUO-induced fibrosis and treatment. **(A)** Images representative of 3 experiments with 20 high-power fields (20×) examined per animal show TUNEL staining of fibrotic kidney tissue alone **(a)** or treatment with laser with or without MSC as follows: **(b)** 635 nm laser, **(c)** 532 nm laser, **(d)** 405 nm laser. **(e)** MSC, **(f)** 635 nm laser with MSC, **(g)** 532 nm laser with MSC, **(h)** 405 nm laser with MSC. **(B)** ANOVA followed by paired *T* tests determined significance as follows: $^{*}p < 0.05$ versus 20 D UUO alone.

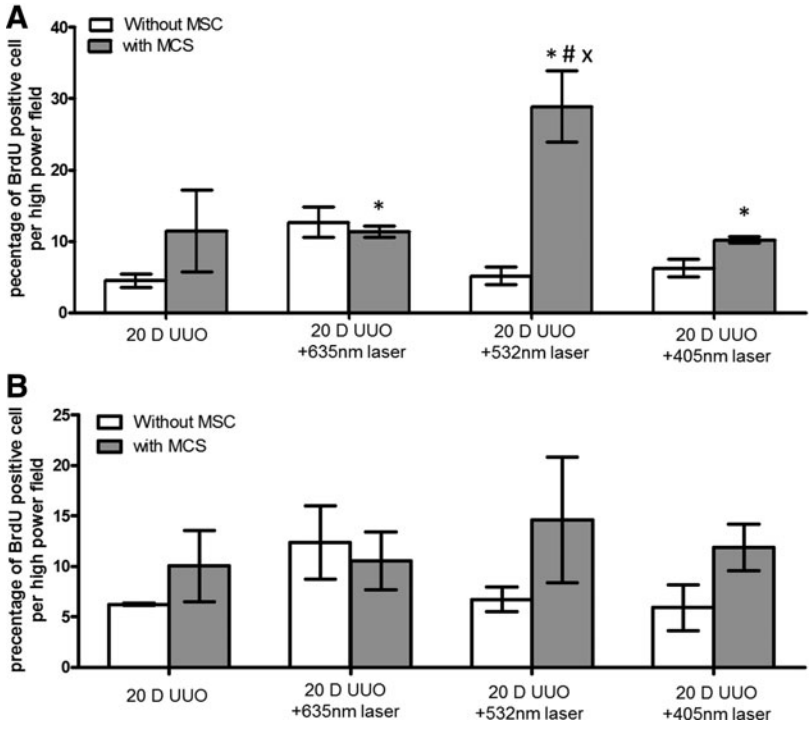

FIG. 3. Proliferative activity identified in the cortex **(A)** or the medulla **(B)** following UUO-induced fibrosis. Percentage of positive BrdU cells per high-power field (20×) is presented as an average of 20 high-power fields per animal. $^{*}p<0.05$ versus 20 D UUO alone, $^{\#}p<0.05$ versus 20 D UUO+ MSC. $^{x}p<0.05$ versus 532 nm laser-treated UUO.

proliferative activity, the frequency of BrdU-positive cells also staining positive for the endothelial marker CD31 was compared to the total number of CD31-positive cells (Fig. 4). In all treatment groups, the percentage of proliferating cells made up less than 1% of the $CD31^{+}$ cells. Of the three laser wavelengths, only the 635 nm wavelength appeared to enhance the endothelial proliferative activity; no synergy was observed with MSC. Addition of MSC synergized with the 405 nm laser ($0.45\% \pm 0.04\%$ vs. $0.24\% \pm 0.03\%$, $p=0.001$ vs. 405 nm alone), which slightly exceeded the 635 nm laser alone ($0.43\% \pm 0.07\%$) and significantly exceeded the D20 UUO control ($0.22\% \pm 0.02\%$, $p=0.005$), and MSC-alone groups ($0.26\% \pm 0.02\%$, $p=0.001$).

The 532 nm wavelength alone or in combination with MSC reduces TGF-β

Since the TGF-β pathway plays a critical role in the perpetuation of renal fibrosis, we investigated whether laser treatment would reduce TGF-β production. Only the 532 nm laser significantly decreased the TGF-β content, (Fig. 5A); the other two laser wavelengths had no appreciable effect. Addition of MSC alone had no effect, however, when combined with the 532 nm laser, there was a significantly greater reduction when compared to MSC treatment alone (354.10 ± 33.11 vs. 1428.00 ± 131.10 pg/mg protein, $p=0.008$)

Since TGF-β can be secreted by tissue macrophages[9] and MSC can convert proinflammatory M1 macrophages to IL-10 secreting M2 macrophages,[39] we examined whether laser treatment in combination with MSC could increase IL-10 production (Fig. 5B). Interestingly, the 635 nm treatment alone demonstrated a strong trend for increased IL-10 when compared to D20 UUO ($14{,}830.00 \pm 633.30$ vs. $18{,}700 \pm 1457.00$ pg/mg protein, $p=0.072$). None of the other treatment groups showed IL-10 increases.

Discussion

Low-level light laser treatments (LLLT) have been used clinically to enhance wound healing through epithelial proliferation and enhanced migration, and to facilitate

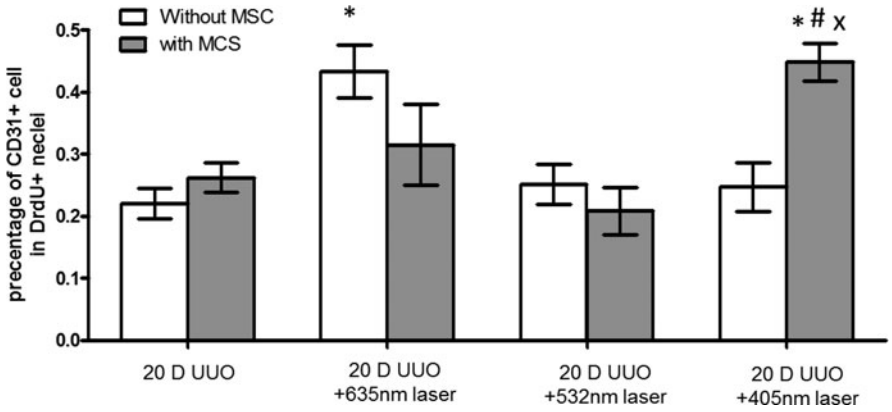

FIG. 4. Endothelial proliferative activity following established fibrosis with UUO. Proliferation endothelial cells were measured by quantification of $CD31^{+}$ endothelial cells staining positive with BrdU and presented as a percentage of all $CD31^{+}$ cells. $^{*}p<0.05$ versus 20 D UUO alone, $^{\#}p<0.05$ versus 20 D UUO+MSC. $^{x}p<0.05$ versus corresponding laser-treated UUO.

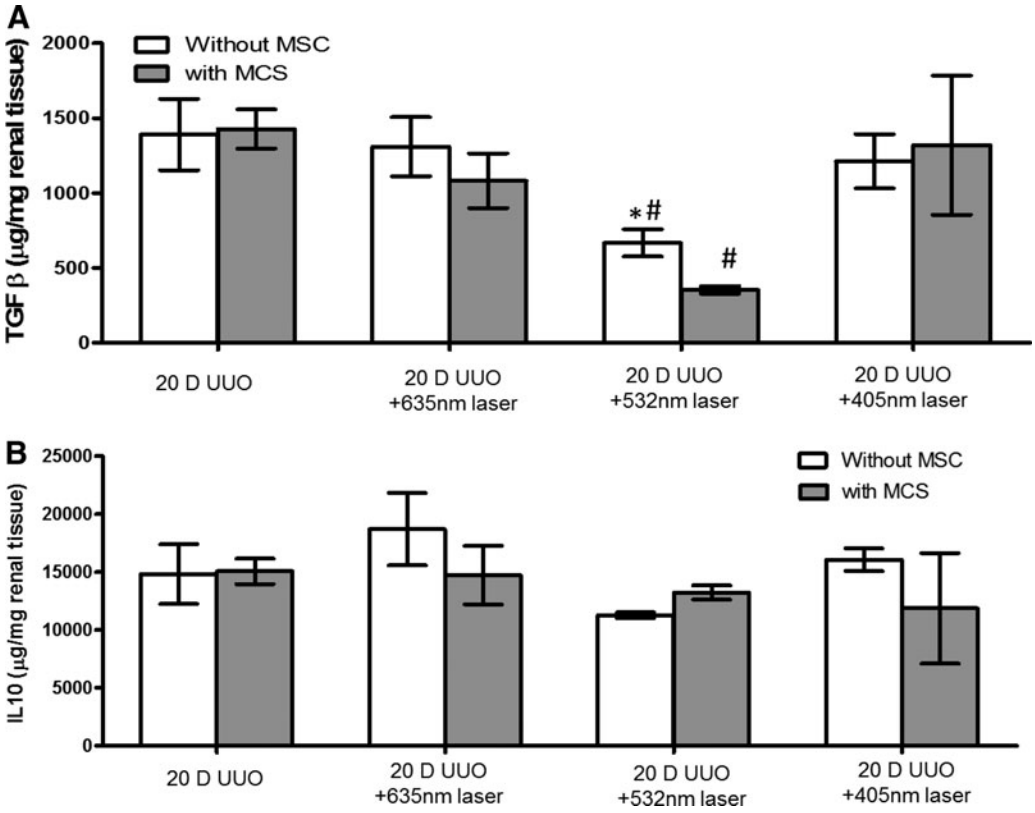

FIG. 5. TGF-β **(A)** and IL10 **(B)** content following UUO-induced fibrosis were measured by ELISA for each explanted fibrotic kidney per treatment type. $^{*}p < 0.05$ versus 20 D UUO alone, $^{\#}p < 0.05$ versus 20 D UUO+MSC. TGF-β, transforming growth factor-β.

healing from musculoskeletal injuries through reduction of inflammation and enhanced proangiogenic activity; LLLT is also being studied for its capacity to enhance neurologic regenerative strategies and for the reduction of inflammatory states.[40–42] Some of these benefits could potentially aid in the reversal of renal fibrosis, a condition in which restoration of normal epithelium, endothelium, and the reduction of ongoing inflammation could impact progression to end-organ failure. In our proof of concept study, we observed that each wavelength had slightly different effects on the features of renal fibrosis, which could be categorized as mitigating mechanisms of fibrosis (apoptosis, TGF-beta production) or enhancing mechanisms of regeneration (mitochondrial activation, proliferation).

Progressive apoptosis has been observed in chronic kidney disease. This finding has been linked to mitochondrial deregulation.[5,43–45] The 635 nm wavelength was the only single-modality treatment group, which enhanced mitochondrial activity at 24 h following administration; addition of MSC to each wavelength led to synergistic effects above that of MSC alone, with the 532 nm and MSC combined treatment group demonstrating greatest gains. When examining reduction of apoptosis, all treatment groups significantly reduced apoptosis at 24 h. These results suggest that MSC synergize with laser to enhance the amount of ATP available to the cell and reduce apoptosis after a single dose of laser energy.

Our findings are in agreement with prior reports that have described enhanced cellular proliferation following exposure to low-level light laser.[46,47] Proliferative effects were observed following a single treatment of 410, 635, or 805 nm, with a maximum mitotic rate between 4 and 8 J/cm^2. Our power density was lower, 2.9 J/cm^2, however, we observed proliferative effects *in vivo*. We observed very low endothelial proliferative activity at this advanced stage of fibrosis. As reported by others,[48] we also observed enhanced endothelial proliferation following LLLT. Endothelial proliferation appeared to increase when MSC were combined with the 405 nm wavelength but not with MSC alone, suggesting that available energy enabled the MSC effect. In the renal cortex, all three wavelengths synergized with MSC to enhance increased BrdU uptake. The 532 nm laser appeared to have the greatest synergistic effect. The cortical region, which exclusively contains the proximal tubule progenitor cells,[44,49] demonstrated the greatest BrdU uptake, suggesting this region as a potential area of investigation. While we cannot definitively conclude our effects specifically targeted proximal tubule progenitor cells without fate mapping studies, the results are encouraging and support more in-depth examination.

Our results were in agreement with prior reports demonstrating the antifibrotic effect of the 532 nm wavelength.[50–52] With a substantive range of power densities, from <1 to 90 J/cm^2 for the 532 nm effect on scar (and presumably TGF-β), it is apparent that additional studies are required to optimize these effects in the setting of renal fibrosis. It is likely that more than one wavelength type at potentially more than one power density will be required to enhance epithelial and endothelial proliferation while

reducing fibrotic activity and apoptosis. Additional studies will be required to determine whether these positive initial effects can be transformed into clinically relevant benefits.

Acknowledgments

This study was supported by the University of Illinois, Department of Surgery. We thank Steve Shanks for the use of research-grade Erchonia lasers for this study.

Author Disclosure Statement

No competing financial interests exist.

References

1. Levey AS, Atkins R, Coresh J, et al. Chronic kidney disease as a global public health problem: approaches and initiatives—a position statement from kidney disease improving global outcomes. Kidney Int 2007;72:247–259.
2. Couser WG, Remuzzi G, Mendis S, Tonelli M. The contribution of chronic kidney disease to the global burden of major noncommunicable diseases. Kidney Int 2011;80: 1258–1270.
3. Zhang G, Oldroyd SD, Huang LH, et al. Role of apoptosis and Bcl-2/Bax in the development of tubulointerstitial fibrosis during experimental obstructive nephropathy. Exp Nephrol 2001;9:71–80.
4. Eddy AA. Progression in chronic kidney disease. Adv Chronic Kidney Dis 2005;12:353–365.
5. Granata S, Zaza G, Simone S, et al. Mitochondrial dysregulation and oxidative stress in patients with chronic kidney disease. BMC Genomics 2009;10:388.
6. Border WA, Noble NA. TGF-beta in kidney fibrosis: a target for gene therapy. Kidney Int 1997;51:1388–1396.
7. Yang J, Liu Y. Dissection of key events in tubular epithelial to myofibroblast transition and its implications in renal interstitial fibrosis. Am J Pathol 2001;159:1465–1475.
8. Lamouille S, Xu J, Derynck R. Molecular mechanisms of epithelial-mesenchymal transition. Nat Rev Mol Cell Biol 2014;15:178–196.
9. Usunier B, Benderitter M, Tamarat R, Chapel A. Management of fibrosis: the mesenchymal stromal cells breakthrough. Stem Cells Int 2014;2014:340257.
10. Yu Y, Lu L, Qian X, et al. Antifibrotic effect of hepatocyte growth factor-expressing mesenchymal stem cells in small-for-size liver transplant rats. Stem Cells Dev 2010; 19:903–914.
11. Zarjou A, Kim J, Traylor AM, et al. Paracrine effects of mesenchymal stem cells in cisplatin-induced renal injury require heme oxygenase-1. Am J Physiol Renal Physiol 2011;300:F254–F262.
12. Bi WR, Xu GT, Lv LX, Yang CQ. The ratio of transforming growth factor-beta1/bone morphogenetic protein-7 in the progression of the epithelial-mesenchymal transition contributes to rat liver fibrosis. Genet Mol Res 2014;13: 1005–1014.
13. Lv S, Liu G, Sun A, et al. Mesenchymal stem cells ameliorate diabetic glomerular fibrosis in vivo and in vitro by inhibiting TGF-beta signalling via secretion of bone morphogenetic protein 7. Diab Vasc Dis Res 2014;11:251–261.
14. Ninichuk V, Gross O, Segerer S, et al. Multipotent mesenchymal stem cells reduce interstitial fibrosis but do not delay progression of chronic kidney disease in collagen4A3-deficient mice. Kidney Int 2006;70:121–129.
15. Duffield JS, Bonventre JV. Kidney tubular epithelium is restored without replacement with bone marrow-derived cells during repair after ischemic injury. Kidney Int 2005; 68:1956–1961.
16. da Silva Meirelles L, Caplan AI, Nardi NB. In search of the in vivo identity of mesenchymal stem cells. Stem Cells 2008;26:2287–2299.
17. Crouch SP, Kozlowski R, Slater KJ, Fletcher J. The use of ATP bioluminescence as a measure of cell proliferation and cytotoxicity. J Immunol Methods 1993;160:81–88.
18. Vander Heiden MG, Cantley LC, Thompson CB. Understanding the Warburg effect: the metabolic requirements of cell proliferation. Science 2009;324:1029–1033.
19. Karu T, Pyatibrat L, Kalendo G. Irradiation with He-Ne laser increases ATP level in cells cultivated in vitro. J Photochem Photobiol B 1995;27:219–223.
20. Kassak P, Przygodzki T, Habodaszova D, Bryszewska M, Sikurova L. Mitochondrial alterations induced by 532 nm laser irradiation. Gen Physiol Biophys 2005;24:209–220.
21. Ferraresi C, Hamblin MR, Parizotto NA. Low-level laser (light) therapy (LLLT) on muscle tissue: performance, fatigue and repair benefited by the power of light. Photonics Lasers Med 2012;1:267–286.
22. Damante CA, De Micheli G, Miyagi SP, Feist IS, Marques MM. Effect of laser phototherapy on the release of fibroblast growth factors by human gingival fibroblasts. Lasers Med Sci 2009;24:885–891.
23. Yu HS, Wu CS, Yu CL, Kao YH, Chiou MH. Helium-neon laser irradiation stimulates migration and proliferation in melanocytes and induces repigmentation in segmental-type vitiligo. J Invest Dermatol 2003;120:56–64.
24. Poon VK, Huang L, Burd A. Biostimulation of dermal fibroblast by sublethal Q-switched Nd:YAG 532 nm laser: collagen remodeling and pigmentation. J Photochem Photobiol B 2005;81:1–8.
25. Alves AN, Fernandes KP, Deana AM, Bussadori SK, Mesquita-Ferrari RA. Effects of low-level laser therapy on skeletal muscle repair: a systematic review. Am J Phys Med Rehabil 2014;93:1073–1085.
26. Sato M, Muragaki Y, Saika S, Roberts AB, Ooshima A. Targeted disruption of TGF-beta1/Smad3 signaling protects against renal tubulointerstitial fibrosis induced by unilateral ureteral obstruction. J Clin Invest 2003;112:1486–1494.
27. Polchert D, Sobinsky J, Douglas G, et al. IFN-gamma activation of mesenchymal stem cells for treatment and prevention of graft versus host disease. Eur J Immunol 2008; 38:1745–1755.
28. Buchwalow IB, Böcker W. Immunochemistry: Basics and Methods. Springer-Verlag Berlin Heidelberg, 2010.
29. Murriel CL, Churchill E, Inagaki K, Szweda LI, Mochly-Rosen D. Protein kinase Cdelta activation induces apoptosis in response to cardiac ischemia and reperfusion damage: a mechanism involving BAD and the mitochondria. J Biol Chem 2004;279:47985–47991.
30. Farrell CL, Bready JV, Rex KL, et al. Keratinocyte growth factor protects mice from chemotherapy and radiation-induced gastrointestinal injury and mortality. Cancer Res 1998;58:933–939.
31. Zeisberg M, Strutz F, Muller GA. Renal fibrosis: an update. Curr Opin Nephrol Hypertens 2001;10:315–320.
32. Maeshima A, Yamashita S, Nojima Y. Identification of renal progenitor-like tubular cells that participate in the

regeneration processes of the kidney. J Am Soc Nephrol 2003;14:3138–3146.
33. Oliver JA, Maarouf O, Cheema FH, Martens TP, Al-Awqati Q. The renal papilla is a niche for adult kidney stem cells. J Clin Invest 2004;114:795–804.
34. Gupta S, Verfaillie C, Chmielewski D, et al. Isolation and characterization of kidney-derived stem cells. J Am Soc Nephrol 2006;17:3028–3040.
35. Morigi M, Imberti B, Zoja C, et al. Mesenchymal stem cells are renotropic, helping to repair the kidney and improve function in acute renal failure. J Am Soc Nephrol 2004;15: 1794–1804.
36. Vogetseder A, Palan T, Bacic D, Kaissling B, Le Hir M. Proximal tubular epithelial cells are generated by division of differentiated cells in the healthy kidney. Am J Physiol Cell Physiol 2007;292:C807–C813.
37. Choi YJ, Chakraborty S, Nguyen V, et al. Peritubular capillary loss is associated with chronic tubulointerstitial injury in human kidney: altered expression of vascular endothelial growth factor. Hum Pathol 2000;31:1491–1497.
38. Kang DH, Hughes J, Mazzali M, Schreiner GF, Johnson RJ. Impaired angiogenesis in the remnant kidney model: II. Vascular endothelial growth factor administration reduces renal fibrosis and stabilizes renal function. J Am Soc Nephrol 2001;12:1448–1457.
39. Nemeth K, Leelahavanichkul A, Yuen PS, et al. Bone marrow stromal cells attenuate sepsis via prostaglandin E(2)-dependent reprogramming of host macrophages to increase their interleukin-10 production. Nat Med 2009; 15:42–49.
40. Kana JS, Hutschenreiter G, Haina D, Waidelich W. Effect of low-power density laser radiation on healing of open skin wounds in rats. Arch Surg 1981;116:293–296.
41. Vasheghani MM, Bayat M, Dadpay M, Habibie M, Rezaei F. Low-level laser therapy using 80-Hz pulsed infrared diode laser accelerates third-degree burn healing in rat. Photomed Laser Surg 2009;27:959–964.
42. Agrawal T, Gupta GK, Rai V, Carroll JD, Hamblin MR. Pre-conditioning with low-level laser (light) therapy: light before the storm. Dose Response 2014;12:619–649.
43. Yuan Y, Chen Y, Zhang P, et al. Mitochondrial dysfunction accounts for aldosterone-induced epithelial-to-mesenchymal transition of renal proximal tubular epithelial cells. Free Radic Biol Med 2012;53:30–43.
44. Manoli I, Sysol JR, Li L, et al. Targeting proximal tubule mitochondrial dysfunction attenuates the renal disease of methylmalonic acidemia. Proc Natl Acad Sci U S A 2013; 110:13552–13557.
45. Chen JF, Liu H, Ni HF, et al. Improved mitochondrial function underlies the protective effect of pirfenidone against tubulointerstitial fibrosis in 5/6 nephrectomized rats. PLoS One 2013;8:e83593.
46. AlGhamdi KM, Kumar A, Moussa NA. Low-level laser therapy: a useful technique for enhancing the proliferation of various cultured cells. Lasers Med Sci 2012;27:237–249.
47. Sroka R, Schaffer M, Fuchs C, et al. Effects on the mitosis of normal and tumor cells induced by light treatment of different wavelengths. Lasers Surg Med 1999;25:263–271.
48. Szymanska J, Goralczyk K, Klawe JJ, et al. Phototherapy with low-level laser influences the proliferation of endothelial cells and vascular endothelial growth factor and transforming growth factor-beta secretion. J Physiol Pharmacol 2013;64:387–391.
49. Lindgren D, Bostrom AK, Nilsson K, et al. Isolation and characterization of progenitor-like cells from human renal proximal tubules. Am J Pathol 2011;178:828–837.
50. Keaney TC, Tanzi E, Alster T. Comparison of 532 nm potassium titanyl phosphate laser and 595 nm pulsed dye laser in the treatment of erythematous surgical scars: a randomized, controlled, open-label study. Dermatol Surg 2016;42:70–76.
51. Cassuto DA, Scrimali L, Sirago P. Treatment of hypertrophic scars and keloids with an LBO laser (532 nm) and silicone gel sheeting. J Cosmet Laser Ther 2010;12:32–37.
52. Cassuto D, Emanuelli G. Non-ablative scar revision using a long pulsed frequency doubled Nd:YAG laser. J Cosmet Laser Ther 2003;5:135–139.

Address correspondence to:
Amelia Bartholomew
Department of Surgery
University of Illinois at Chicago
Chicago, IL 60612

E-mail: ambart@uic.edu

Received: November 1, 2015.
Accepted after revision: March 22, 2016.
Published online: May 31, 2016.